

Analysis of circular torsion bar with circular holes using null-field approach

Wen-Cheng Shen[†], Po-Yuan Chen[†], Jeng-Tzong Chen[‡]

Keywords: Null-field integral equation, degenerate kernel, Fourier series, circular holes, torsional rigidity

Abstract

The degenerate kernels and Fourier series expansions are adopted in the null-field integral equation to solve torsion problems of a circular bar with circular holes. The main gain of using degenerate kernels is free of calculating the principal values. An adaptive observer system is addressed to fully employ the property of degenerate kernels in the polar coordinate. After moving the null-field point to the boundary and matching the boundary conditions, a linear algebraic system is obtained without boundary discretization. The unknown coefficients in the algebraic system can be easily determined. The present method is treated as a “semi-analytical” solution since error only attributes to the truncation of Fourier series. Finally, several examples are given to demonstrate the validity of the proposed method.

零場方程求解含多圓洞之圓桿扭轉分析

沈文成[†] 陳柏源[†] 陳正宗[‡]

關鍵字：零場積分方程、分離核函數、傅立葉級數、圓孔洞、抗扭剛度

摘要

本文使用零場積分方程搭配分離核函數與傅立葉級數求解含圓形邊界之扭轉問題。藉由分離核函數的表示式，可解析計算所有的邊界積分而免於計算主值的困擾。文中採用自適性觀察座標系統的想法，來充分掌握分離核函數的特性。透過零場積分方程將零場點推向邊界且均勻佈點，滿足邊界條件後可以得到一線性代數方程式，其中的未知傅立葉係數均可輕易地求得。由於誤差僅來自於擷取有限項的傅立葉級數，故本方法可視為“半解析法”。最後，為了驗證此方法的可行性與正確性，提出含圓孔洞的受扭桿問題予以測試。

[†] Graduate student, Department of Harbor and River Engineering, National Taiwan Ocean University

[‡] Distinguished Professor, Department of Harbor and River Engineering, National Taiwan Ocean University

1 Introduction

Boundary value problem always involve several holes or more than one important point. It is convenient to be able to expand the solutions in alternative ways, each way referring to different specific coordinate set describing the same solution. According to the idea, we develop the adaptive observer system and expanded form of fundamental solution which is called “degenerate kernel” in the polar coordinate and employ Fourier series to approximate the boundary data.

In the past, multiply connected problems have been carried out either by conformal mapping or by special technique approach. Muskhelishvili [1] has formulated the solution of composite torsion bar in the form of integral equations. He solved the problem of a circular bar reinforced by an eccentric inclusion by using conformal mapping. Chen and Weng [2] have also introduced conformal mapping with a Laurent series expansion to analyze the Saint-Venant torsion problem. They concerned with a nonconcentric circular bar of different materials with an imperfect interface under torque. Because the conformal mapping is limited to the doubly connected region, an increasing number of researchers have paid more attentions on special solutions. However, the extension of above special solution to multiple circular holes may encounter difficulty. It is not trivial to develop a systematic method for solving the torsion problems with several holes.

In this paper, the null-field integral equation is utilized to solve the Saint-Venant torsion problem of a circular shaft weakened by

circular holes. The mathematical formulation is derived by using degenerate kernel for fundamental solution and Fourier series for boundary density in the null-field integral equation. Then, it reduces to a linear algebraic equation. After determining the unknown coefficients, series solutions for the warping function and torsional rigidity are obtained. Numerical examples are given to show the validity and efficiency of our formulation.

2 Solution procedures

2.1 Dual boundary integral equations and dual null-field integral equations

What is given shown in Figure 1 is a circular bar weakened by N circular holes placed on a concentric ring of radius b . The radii of the outer circle and the inner holes are R and a , respectively. The circular bar twisted by couples applied at the ends is taken into consideration.

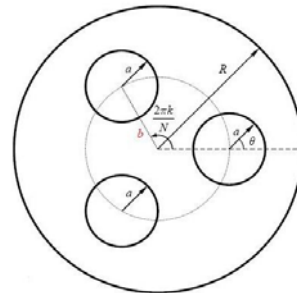


Figure 1 Cross section of bar weakened by N ($N = 3$) equal circular holes

The classical Saint-Venant torsion problem is formulated as Laplace equation $\nabla^2\varphi = 0$ subject to the Neumann boundary condition

$$\frac{\partial\varphi}{\partial n} = x_k \sin\theta_k - y_k \cos\theta_k, \quad (1)$$

where φ is the warping function, (x_k, y_k)

denotes the center of the k th inner circular hole defined as

$$x_k = b \cos \frac{2\pi k}{N}, \quad y_k = b \sin \frac{2\pi k}{N}, \quad (2)$$

$$k = 1, 2, \dots, N.$$

We apply the Fourier series expansions to approximate the potential u and its normal derivative t on the boundary

$$u(s_k) = a_0^k + \sum_{n=1}^{\infty} (a_n^k \cos n\theta_k + b_n^k \sin n\theta_k), \quad (3)$$

$$s_k \in B_k, \quad k = 1, 2, \dots, N,$$

$$t(s_k) = p_0^k + \sum_{n=1}^{\infty} (p_n^k \cos n\theta_k + q_n^k \sin n\theta_k), \quad (4)$$

$$s_k \in B_k, \quad k = 1, 2, \dots, N,$$

where $t(s_k) = \partial u(s_k) / \partial \mathbf{n}_s$ in which \mathbf{n}_s and denotes the outward normal vector at the source point s , a_n^k , b_n^k , p_n^k and q_n^k ($n=0, 1, 2, \dots$) are the Fourier coefficients and θ_k is the polar angle. The integral equation for the domain point can be derived from the third Green's identity [3], we have

$$2\pi u(x) = \int_B T(s, x) u(s) dB(s) - \int_B U(s, x) t(s) dB(s), \quad x \in D, \quad (5)$$

where s and x are the source and field points, respectively, B is the boundary, D is the domain of interest, and the kernel function $U(s, x) = \ln r$, ($r \equiv |x-s|$), is the fundamental solution which satisfies

$$\nabla^2 U(s, x) = 2\pi \delta(x-s), \quad (6)$$

in which $\delta(x-s)$ denotes the Dirac-delta function. The $T(s, x)$ kernel is defined by

$$T(s, x) \equiv \frac{\partial U(s, x)}{\partial \mathbf{n}_s}, \quad (7)$$

By collocating x outside the domain ($x \in D^c$), we obtain the dual null-field integral equations as shown below

$$0 = \int_B T(s, x) u(s) dB(s) - \int_B U(s, x) t(s) dB(s), \quad x \in D^c, \quad (8)$$

where D^c is the complementary domain. Based on the separable property, the kernel function $U(s, x)$ can be expanded into degenerate form by separating the source points and field points in the polar coordinate [4]:

$$U(s, x) = \begin{cases} U^i(R, \theta; \rho, \phi) = \\ \ln R - \sum_{m=1}^{\infty} \frac{1}{m} \left(\frac{\rho}{R}\right)^m \cos m(\theta - \phi), \quad R \geq \rho \\ U^e(R, \theta; \rho, \phi) = \\ \ln \rho - \sum_{m=1}^{\infty} \frac{1}{m} \left(\frac{R}{\rho}\right)^m \cos m(\theta - \phi), \quad \rho > R \end{cases}, \quad (9)$$

where the superscripts “ i ” and “ e ” denote the interior ($R > \rho$) and exterior ($\rho > R$) cases, respectively. After taking the normal derivative with respect to Eq. (9), the $T(s, x)$ kernel function can be derived as

$$T(s, x) = \begin{cases} T^i(R, \theta; \rho, \phi) = \\ \frac{1}{R} + \sum_{m=1}^{\infty} \left(\frac{\rho^m}{R^{m+1}}\right) \cos m(\theta - \phi), \quad R > \rho \\ T^e(R, \theta; \rho, \phi) = \\ -\sum_{m=1}^{\infty} \left(\frac{R^{m-1}}{\rho^m}\right) \cos m(\theta - \phi), \quad \rho > R \end{cases}, \quad (10)$$

Since the potential resulted from $T(s, x)$ is discontinuous cross the boundary, the potentials of $T(s, x)$ for $R \rightarrow \rho^+$ and $R \rightarrow \rho^-$ are different. This is the reason why $R = \rho$ is not included in expressional degenerate kernels of $T(s, x)$ in Eq. (10).

2.2 Adaptive observer system

After moving the point of Eq. (8) to the boundary, the boundary integrals through all the circular contours are required. Since the boundary integral equations are frame

indifferent, *i.e.* objectivity rule, the observer system is adaptively to locate the origin at the center of circle in the boundary integrals. Adaptive observer system is chosen to fully employ the property of degenerate kernels. Figures 2 (a) and 2 (b) show the boundary integration for the circular boundaries in the adaptive observer system. It is worthy noted that the origin of the observer system is located on the center of the corresponding circle under integration to entirely utilize the geometry of circular boundary for the expansion of degenerate kernels and boundary densities.

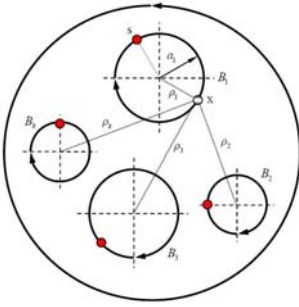


Figure 2 (a) Null-field integral equation

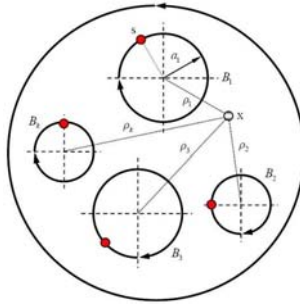


Figure 2 (b) Boundary integral equation for domain points

2.3 Linear algebraic system

By moving the null-field point x_k on the k th circular boundary in the sense of limit for Eq. (8) in Figure 2 (a), we have

$$0 = \sum_{k=1}^{N_c} \int_{B_k} T(s_k, x_j) u(s_k) dB_k(s) - \sum_{k=1}^{N_c} \int_{B_k} U(s_k, x_j) t(s_k) dB_k(s), \quad x \in D^c, \quad (11)$$

where N_c is the number of circles including the outer boundary and the inner circular holes. If the domain is unbounded, the outer boundary B_0 is a null set and $N_c = N$. By collocating the null-field point

on the boundary, a linear algebraic system is obtained

$$[\mathbf{U}]\{\mathbf{t}\} = [\mathbf{T}]\{\mathbf{u}\}, \quad (12)$$

where $[\mathbf{U}]$ and $[\mathbf{T}]$ are the influence matrices with a dimension of $N_c(2M+1)$ by $N_c(2M+1)$, $\{\mathbf{u}\}$ and $\{\mathbf{t}\}$ denote the column vectors of Fourier coefficients with a dimension of $N_c(2M+1)$ by 1 in which $[\mathbf{U}]$, $[\mathbf{T}]$, $\{\mathbf{u}\}$ and $\{\mathbf{t}\}$ can be defined as follows:

$$[\mathbf{U}] = \begin{bmatrix} U_{00} & U_{01} & \dots & U_{0N} \\ U_{10} & U_{11} & \dots & U_{1N} \\ \vdots & \vdots & \ddots & \vdots \\ U_{N0} & U_{N1} & \dots & U_{NN} \end{bmatrix}, [\mathbf{T}] = \begin{bmatrix} T_{00} & T_{01} & \dots & T_{0N} \\ T_{10} & T_{11} & \dots & T_{1N} \\ \vdots & \vdots & \ddots & \vdots \\ T_{N0} & T_{N1} & \dots & T_{NN} \end{bmatrix}, \quad (13)$$

$$\{\mathbf{u}\} = \begin{bmatrix} u_0 \\ u_1 \\ u_2 \\ \vdots \\ u_N \end{bmatrix}, \quad \{\mathbf{t}\} = \begin{bmatrix} t_0 \\ t_1 \\ t_2 \\ \vdots \\ t_N \end{bmatrix}, \quad (14)$$

where the vectors $\{\mathbf{u}_k\}$ and $\{\mathbf{t}_k\}$ are in the form of $\{a_0^k \ a_1^k \ b_1^k \ \dots \ a_M^k \ b_M^k\}^T$ and $\{p_0^k \ p_1^k \ q_1^k \ \dots \ p_M^k \ q_M^k\}^T$, respectively; the first subscript “ j ” ($j = 0, 1, 2, \dots, N$) in $[\mathbf{U}_{jk}]$ and $[\mathbf{T}_{jk}]$ denotes the index of the j th circle where the collocation point is located and the second subscript “ k ” ($k = 0, 1, 2, \dots, N$) denotes the index of the k th circle where boundary data $\{\mathbf{u}_k\}$ or $\{\mathbf{t}_k\}$ are specified, M indicates the truncated terms of Fourier series. By rearranging the known and unknown sets, the unknown Fourier coefficients are determined. Equation (8) can be calculated by employing the relations of trigonometric function and the orthogonal property in the real computation. Only the finite M terms are used in the summation of Eqs. (3) and (4).

3 Illustrative examples

Case 1: A circular bar with single eccentric hole

A circular bar of radius R with two equal circular holes removed is under torque T at the end. The torsional rigidity G of cross section can be expressed by

$$\frac{G}{\mu} = \int_D r^2 dA - \sum_{k=1}^N \int_{B_k} \varphi \frac{\partial \varphi}{\partial n} dB_k, \quad (15)$$

where μ is the elastic shear modulus. The results of torsional rigidity for each case are shown in Table 1. The exact solution derived by Muskhelishvili [1] is shown in Table 1 for comparison. For the eccentric hole near the outer boundary, our solution is better than that of Caulk obtained by BIE [5].

Table 1 Torsional rigidity of a circular cylinder with a single eccentric hole ($a/R = 1/3$)

| $\frac{b}{R-a}$ | $2G / \mu\pi R^4$ | | |
|-----------------|-------------------|--------------------|---------|
| | Present method | Exact solution [1] | BIE [5] |
| 0.20 | 0.97872 | 0.97872 | 0.97872 |
| 0.40 | 0.95137 | 0.95137 | 0.95137 |
| 0.60 | 0.90312 | 0.90312 | 0.90316 |
| 0.80 | 0.82473 | 0.82473 | 0.82497 |
| 0.90 | 0.76168 | 0.76168 | 0.76252 |
| 0.92 | 0.74455 | 0.74454 | 0.74569 |
| 0.94 | 0.72451 | 0.72446 | 0.72605 |
| 0.96 | 0.69991 | 0.69968 | 0.70178 |
| 0.98 | 0.66705 | 0.66555 | 0.66732 |

Case 2: A circular bar with two circular holes

What is brought out is the problem subject to zero traction on the outer boundary and Neumann boundary condition defined in Eq.(1) on all the inner circles. Figures 3 (a)

and 3 (b) show the results using the present method and those from the first-order approximation solution (solid lines) and the boundary integral equation solution (dashed lines) derived by Caulk [5]. Twenty-one collocating points are selected on all the circular boundaries in the numerical implementation. After being compared with the results of Figure 3 (b), the numerical results match well with other solutions.

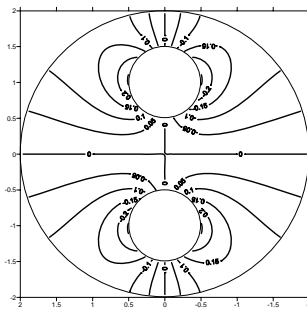


Figure 3 (a) Contour plot of present method

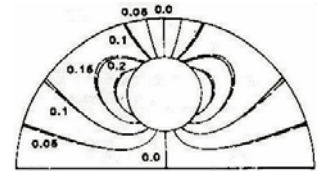


Figure 3 (b) Caulk's data

Case 3: A circular bar with three circular holes

Unlike Case 2, a circular bar weakened by three circular holes of equal radii is regarded as the third example. In a similar way, the contour plot of the axial displacement is shown in Figure 4 (a). Good agreement is made after comparing with the Caulk's data in Figure 4 (b).

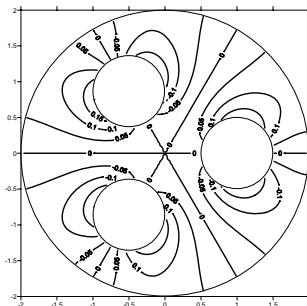


Figure 4 (a) Contour plot of the present method

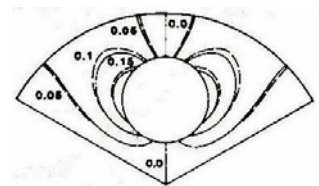


Figure 4 (b) Caulk's data

Case 4: A circular bar with four circular holes

The fourth problem is a circular bar weakened by four equal circular holes under torque. In Figure 5 (a), our results of axial displacement agree well with the values in the dashed line of Figure 5 (b) which are solved by using the boundary integral equation.

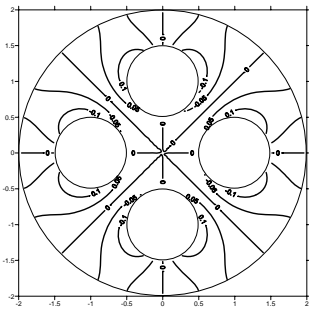


Figure 5 (a) Contour plot of the present method

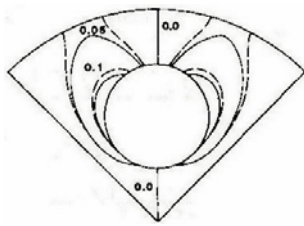


Figure 5 (b) Caulk's data

The torsional rigidities obtained by using the present method for $N = 2, 3, 4$ are listed in Table 2. Our results are consistent with Caulk's data obtained by BIE formulation after comparison.

Table 2 Torsional rigidity of a circular cylinder with a ring of N holes ($a/R = 1/4, b/R = 1/2$)

| $2G / \mu\pi R^4$ | | | |
|-------------------|----------------|---------|--------------------------|
| Numbers of holes | Present method | BIE [5] | First-order solution [5] |
| 2 | 0.8657 | 0.8657 | 0.8661 |
| 3 | 0.8214 | 0.8214 | 0.8224 |
| 4 | 0.7893 | 0.7893 | 0.7934 |

4 Concluding remarks

The torsion problems of circular shaft weakened by several holes have been successfully solved by using the present formulation. Our solutions are consistent

with the results by using the boundary integral equation for the three cases of Caulk's. After being compared with the exact solution in the case of an eccentric hole and Caulk's data, our results show the better efficiency and accuracy.

References

- 1 Muskhelishvili NI (1953), *Some basic problems of the mathematical theory of elasticity*, Noordhoff, Groningen.
- 2 Chen T and Weng IS (2001), "Torsion of a circular compound bar with imperfect interface", *Journal of Applied Mechanics, ASME*, **68**, 955-958.
- 3 Chen JT, Hong H-K (1999), "Review of dual boundary element methods with emphasis on hypersingular integrals and divergent series", *Applied Mechanics Reviews, ASME*, **52**, 17-33.
- 4 Chen JT, Chiu YP (2002), "On the pseudo-differential operators in the dual boundary integral equations using degenerate kernels and circulants", *Engineering Analysis with Boundary Elements*, **26**, 41-53.
- 5 Caulk DA (1983), "Analysis of elastic torsion in a bar with circular holes by a special boundary integral method", *Journal of Applied Mechanics, ASME*, **50**, 101-108.
- 6 Chen JT, Shen WC and Wu AC (2005), "Null-field integral equations for stress field around circular holes under anti-plane shear", *Engineering Analysis with Boundary Elements*, Revised.